MHD flow and heat transfer in a non-Newtonian liquid film over an unsteady stretching sheet with variable fluid properties

Mostafa A.A. Mahmoud and Ahmed M. Megahed

Abstract: The present paper is concerned with the study of variable viscosity and variable thermal conductivity on the flow and heat transfer of an electrically conducting non-Newtonian power-law fluid within a thin liquid film over an unsteady stretching sheet in the presence of a transverse magnetic field. The transformed system of nonlinear ordinary differential equations describing the problem is solved numerically. The effects of various parameters on the velocity and temperature profiles are shown through graphs and discussed. The values of the local skin-friction coefficient and the local Nusselt number for different values of physical parameters are presented through tables.

PACS Nos: 47.50.–d, 47.15.gm

Résumé : Nous étudions ici les effets d'une viscosité et d'une conductivité thermique variables sur l'écoulement et le transfert de chaleur d'un fluide non Newtonien conducteur à l'intérieur d'un mince film liquide sur une surface instable élastique en présence d'un champ magnétique transverse. Le système transformé d'équations différentielles ordinaires non linéaires est alors solutionné numériquement. Nous présentons de façon graphique et analysons les résultats illustrant les effets des différents paramètres sur les profils de vitesse et de température. Nous présentons sous forme de tables les valeurs du coefficient local de friction de peau et du nombre local de Nusselt pour différentes valeurs des paramètres physiques.

[Traduit par la Rédaction]

1. Introduction

The study of fluid flow and heat transfer in a thin liquid film over an unsteady stretching surface has gained considerable attention due to its many theoretical and technical applications in the engineering and technology fields. The knowledge of heat transfer within a thin liquid film is crucial in understanding the coating process and design of various heat exchangers and chemical-processing equipment. Some applications include reactor fluidization, wire and fiber coating, polymer processing, food-stuff processing, transpiration cooling; etc. Many metallurgical processes, such as drawing, annealing, and tinning of copper wires involve cooling of continuous strips or filaments by drawing them through a quiescent fluid. The quality of the final product depends on the rate of heat transfer at the stretching surface. Wang [1] was the first who studied the flow of a Newtonian fluid in a thin liquid film over an unsteady stretching sheet. Later Andersson et al. [2] extended Wang's problem to the case of heat transfer. Dandapat et al. [3] investigated the effect of the thermocapillarity on the flow and heat transfer in a thin liquid film over an unsteady stretching sheet. Liu and Andersson [4] generalized the analysis by Andersson et al. [2] by considering a more general form of the prescribed temperature variation of the stretching sheet that is considered in ref. 2. The combined effect of viscous dissipation and magnetic field on the flow and heat transfer in a liquid film over an unsteady stretching surface was studied by Subhas Abel et al. [5]. In the studies mentioned above [1–5], the fluid was assumed to be Newtonian. Many materials such as polymer solutions or melts, drilling mud, certain oils, greases, pulps, fossil fuels; etc. are classified as a non-Newtonian fluids due to the nonlinearity in the relationship between the stress and the rate of the strain of these fluids. Many of the non-Newtonian fluids used in the chemical engineering follow the Ostwald-de Waele power-law model for the shear stress. Andersson et al. [6] examined, numerically, the problem of hydrodynamic power-law fluid flow within a liquid thin film over a stretching sheet. Chen [7] studied the heat transfer occurring in a thin liquid film of a power-law fluid over an unsteady stretching sheet. Wang and Pop [8] analytically studied the flow of a power-law fluid film on an unsteady stretching surface by means of the homotopy analysis method. Hayat et al. [9] investigated magneto-hydrodynamic (MHD) flow and heat transfer of a second-grade fluid film over an unsteady stretching sheet. Siddiqui et al. [10] studied the thin film flow of two non-Newtonian fluids, namely, a Sisko fluid and an Oldroyd 6-constant fluid on a vertical moving belt. The effect of viscous dissipation on heat transfer in a non-Newtonian power-law liquid in a thin film over an unsteady stretching surface has been studied by Chen [11]. The above studies are discussed in the case of constant fluid properties. Particularly, the physical properties change significantly with temperature. Therefore, it is necessary to take the variation of viscosity and thermal conductivity into consideration. Dandapat et al. [12] discussed the ef-

Received 1 May 2009. Accepted 26 June 2009. Published on the NRC Research Press Web site at cjp.nrc.ca on 1 December 2009.

M.A.A. Mahmoud[1] and A.M. Megahed. Department of Mathematics, Faculty of Science, Benha University (13518), Egypt.

[1]Corresponding author (e-mail: mostafabdelhameed@yahoo.com).

Fig. 1. Schematic of the physical system.

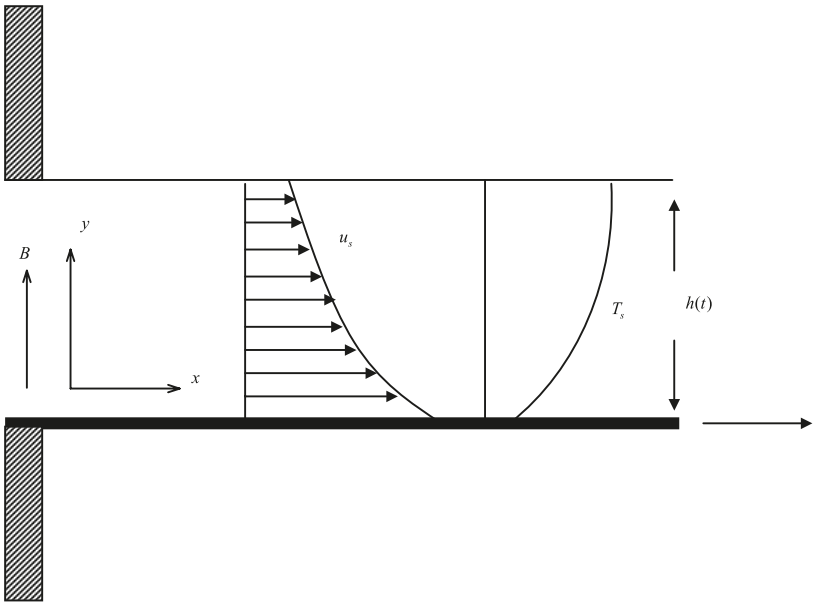

fects of variable viscosity, variable thermal conductivity, and thermocapillarity on the flow and heat transfer within a Newtonian thin liquid film over an unsteady stretching sheet. The viscosity is assumed to vary exponentially with the temperature [13, 14] and the thermal conductivity is assumed to vary linearly with the temperature [15–19]. In the present study, we investigate the effects of a transverse magnetic field on the flow and heat transfer of a non-Newtonian power-law fluid film over an unsteady stretching surface in the presence of variable viscosity and variable thermal conductivity.

2. Formulation of the problem

Consider the unsteady flow of an electrically conducting non-Newtonian power-law fluid in a thin liquid film over a stretching surface. The elastic sheet issues from a narrow slit at the origin of a Cartesian coordinate system as shown in Fig. 1. The continuous surface aligned with the x-axis at $y = 0$ moves in its own plane with a velocity $u_s(x, t)$ and temperature distribution $T_s(x, t)$. A thin liquid film of uniform thickness $h(t)$ lies on the horizontal surface. A magnetic field is applied along the y-axis normal to the surface and the effect of the induced magnetic field induced by the motion of the fluid in the presence of a transverse magnetic field is neglected. The basic equations in the thin liquid layer are governed by the two-dimensional boundary layer equations for mass, momentum, and energy [11], they are

$$\frac{\partial u}{\partial x} + \frac{\partial v}{\partial y} = 0 \tag{1}$$

$$\frac{\partial u}{\partial t} + u\frac{\partial u}{\partial x} + v\frac{\partial u}{\partial y} = \frac{1}{\rho}\frac{\partial}{\partial y}(\tau_{xy}) - \frac{\sigma B^2}{\rho}u \tag{2}$$

$$\frac{\partial T}{\partial t} + u\frac{\partial T}{\partial x} + v\frac{\partial T}{\partial y} = \frac{1}{\rho c_p}\frac{\partial}{\partial y}\left(\kappa\frac{\partial T}{\partial y}\right) \tag{3}$$

where τ_{xy} is the shear stress, in the present problem we have $\partial u/\partial y < 0$, this gives the shear stress as

$$\tau_{xy} = -K\left(-\frac{\partial u}{\partial y}\right)^n \tag{4}$$

where K is the consistency coefficient and n is the power-law index. The fluid is Newtonian for $n = 1$ with $K = \mu$. $n < 1$ and $n > 1$ corresponds to pseudo-plastic (or shear thinning) and dilatant (or shear thickening) fluids, respectively. u and v are the components along the x and y directions, respectively. ρ is the density of the fluid, T is the temperature of the fluid, σ is the electrical conductivity, B is the strength of the applied magnetic field, κ is the thermal conductivity, and c_p is the specific heat at constant pressure.

The appropriate boundary conditions for the present problem are

$$u = u_s, \qquad v = 0, \qquad T = T_s \quad \text{at} \quad y = 0 \tag{5}$$

$$\frac{\partial u}{\partial y} = \frac{\partial T}{\partial y} = 0 \quad \text{at} \quad y = h \tag{6}$$

$$v = \frac{\partial h}{\partial t} + u\frac{\partial h}{\partial x} \quad \text{at} \quad y = h \tag{7}$$

where u_s is the surface velocity of the stretching sheet and the flow is caused by stretching the elastic surface at $y = 0$ such that the continuous sheet moves in the x-direction with the velocity

$$u_s = \frac{bx}{1 - at} \tag{8}$$

where h is the thickness of the liquid film. a and b are positive constants with dimension (time)$^{-1}$. T_s the surface temperature of the stretching sheet varies with the distance x along the sheet and time t in the form

$$T_s = T_0 - T_{\text{ref}}\left[\frac{b^{2-n}x^2}{2(K_0/\rho)}\right](1 - at)^{n-(5/2)} \tag{9}$$

where T_0 is the fluid temperature at the slit (constant) and

$T_{ref} = T_0$ [2, 4]. As per mathematical requirement, $t < 1/a$ in (8) and (9), on which the following analysis is based [2, 9]. The applied transverse magnetic field is assumed to be in the form

$$B(t) = B_0(1 - at)^{-1/2} \tag{10}$$

Now we define the following dimensionless variables:

$$\eta = \left[\frac{b^{2-n}}{(K_0/\rho)}\right]^{1/(n+1)} x^{(1-n)/(1+n)}(1 - at)^{(n-2)/(n+1)} y \tag{11}$$

$$\psi = \left[\frac{b^{1-2n}}{(K_0/\rho)}\right]^{-1/(n+1)} x^{2n/(1+n)}(1 - at)^{(1-2n)/(n+1)} f \tag{12}$$

$$T = T_0 - T_0\left[\frac{b^{2-n}x^2}{2(K_0/\rho)}\right](1 - at)^{n-(5/2)}\theta \tag{13}$$

where ψ is the stream function that satisfies the continuity equation (1), f is the dimensionless stream function and

$$\theta = \frac{(T - T_0)}{(T_s - T_0)}$$

is the dimensionless temperature of the fluid. The consistency coefficient K and the thermal conductivity κ, which are given as [12]

$$K = K_0\, e^{\alpha\theta} \tag{14}$$

$$\kappa = \kappa_0(1 + \varepsilon\theta) \tag{15}$$

where K_0 and κ_0 are the consistency coefficient and thermal conductivity at the slit temperature T_0. α is the viscosity parameter and ε is the thermal conductivity parameter. Substituting the transformation given in (11–13) and using (14) and (15) one obtains the following non-dimensional equations governing the flow, the energy, and the boundary conditions

$$e^{\alpha\theta}(nf''^{n-1}f''' + \alpha\theta' f''^{n}) + \frac{2n}{n+1}ff'' - f'^2 - S\left[f' + \left(\frac{2-n}{1+n}\right)\eta f''\right] - Mf' = 0 \tag{16}$$

$$\frac{1}{Pr}[(1 + \varepsilon\theta)\theta'' + \varepsilon\theta'^2] + \left(\frac{2n}{n+1}\right)f\theta' - 2f'\theta - S\left[\left(\frac{5}{2} - n\right)\theta + \left(\frac{2-n}{1+n}\right)\eta\theta'\right] = 0 \tag{17}$$

$$f = 0, \qquad f' = 1, \qquad \theta = 1 \quad \text{at} \quad \eta = 0 \tag{18}$$

$$f'' = 0, \qquad \theta' = 0 \quad \text{at} \quad \eta = \beta \tag{19}$$

$$f = \left(\frac{2-n}{2n}\right)S\beta \quad \text{at} \quad \eta = \beta \tag{20}$$

where a prime denotes differentiation with respect to η, $S = a/b$ is the unsteadiness parameter, $Pr = (\rho c_p/\kappa_0)xu_s Re_x^{-2/(n+1)}$ is the generalized Prandtl number, $M = \sigma B_0^2/\rho b$ is the magnetic number and β denotes the value of η at the free surface.

The physical quantities of interest are the local skin-friction coefficient C_{fx} and the local Nusselt number Nu_x, which are defined as

$$C_{fx} = 2\,Re_x^{-1/(n+1)}\, e^{\alpha}[-f''(0)]^n \tag{21}$$

$$Nu_x = -Re_x^{1/(n+1)}\theta'(0) \tag{22}$$

where $f''(0) < 0$ otherwise $(-f''(0))^n$ will not be real for fractional n and $Re_x = \rho u_s^{2-n}x^n/K_0$ is the local Reynolds number.

3. Numerical solution

The coupled system of nonlinear ordinary differential equations (16) and (17) with the boundary conditions (18)–(20) is solved numerically using the most efficient numerical shooting technique with the fourth-order Runge–Kutta scheme. We set

$$y_1 = f, \qquad y_2 = y_1', \qquad y_3 = y_2', \qquad y_4 = \theta, \qquad y_5 = y_4' \tag{23}$$

Equations (16) and (17) then reduced to a system of a first-order ordinary differential equations; i.e.,

$$\begin{aligned}
&y_1' = y_2, \qquad y_1(0) = 0, \qquad y_2' = y_3, \qquad y_2(0) = 1, \qquad y_4' = y_5, \qquad y_4(0) = 1\\
&y_3' = \frac{1}{n}|y_3|^{1-n}\left(-\alpha y_5 y_3^n + e^{-\alpha y_4}\left\{\frac{-2n}{n+1}y_1y_3 + y_2^2 + S\left[y_2 + \left(\frac{2-n}{1+n}\right)\eta y_3\right] + My_2\right\}\right), \qquad y_3(0) = \epsilon_1\\
&y_5' = \frac{1}{1+\varepsilon y_4}\left(-\varepsilon y_5^2 + Pr\left\{\frac{-2n}{n+1}y_1y_5 + 2y_2y_4 + S\left[\left(\frac{5}{2} - n\right)y_4 + \left(\frac{2-n}{1+n}\right)\eta y_5\right]\right\}\right), \qquad y_5(0) = \epsilon_2
\end{aligned} \tag{24}$$

The shooting method is used to guess ϵ_1 and ϵ_2 by iterations until the outer boundary conditions (19) are satisfied. The estimated value of β is, therefore, systematically adjusted until (20) is satisfied to within 10^{-6}. Once the convergence in achieved, the resulting differential equations can be integrated using a fourth-order Runge–Kutta integration scheme. The above procedure is repeated until we get the results up to the desired degree of accuracy, 10^{-5}. To assess the accuracy of the present method, results for our problem in the absence of magnetic field ($M = 0$), constant fluid viscosity ($\alpha = 0$), and constant fluid thermal conductivity ($\varepsilon = 0$) are compared with those obtained by Chen [11] as shown in Table 1. It was found that our results agree very well with those of Chen [11].

Table 1. Comparison for values of $f''(0)$ and β with $Pr = 10$, $S = 0.8$, and $S = 1.2$.

		β		$f''(0)$	
S	n	Chen [11]	Present work	Chen [11]	Present work
0.8	0.8	1.3266	1.3266	–1.22301	–1.22302
1.2	0.8	0.4326	0.43261	–0.77919	–0.77918
0.8	1	2.1520	2.1520	–1.24581	–1.24581
1.2	1	1.1278	1.1278	–1.27918	–1.27917
0.8	1.2	3.0306	3.03061	–1.21778	–1.21778
1.2	1.2	1.8276	1.8277	–1.30883	–1.30883

Fig. 2. (*a*) Velocity distribution for various values of n with $S = 0.8$. (*b*) Velocity distribution for various values of n with $S = 1.2$.

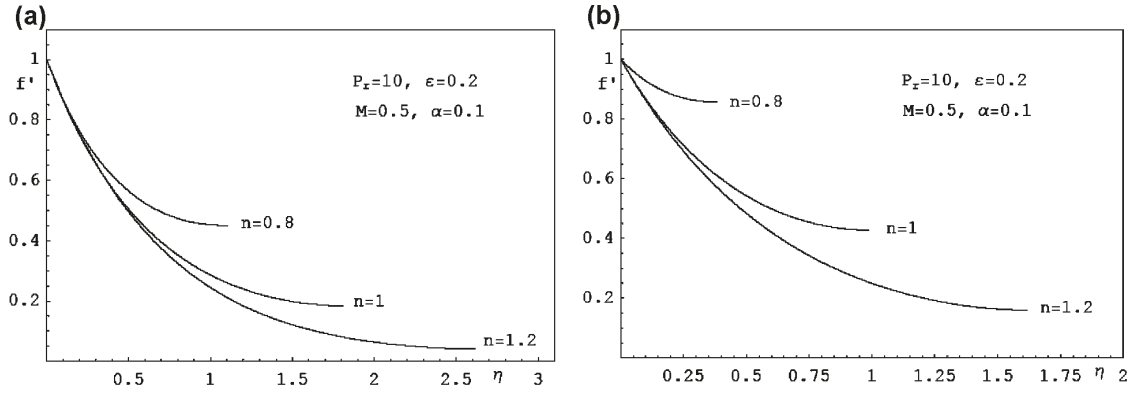

Fig. 3. (*a*) Velocity distribution for various values of α with $n = 0.8$. (*b*) Velocity distribution for various values of α with $n = 1.2$. (*c*) Velocity distribution for various values of α with $n = 0.8$. (*d*) Velocity distribution for various values of α with $n = 1.2$.

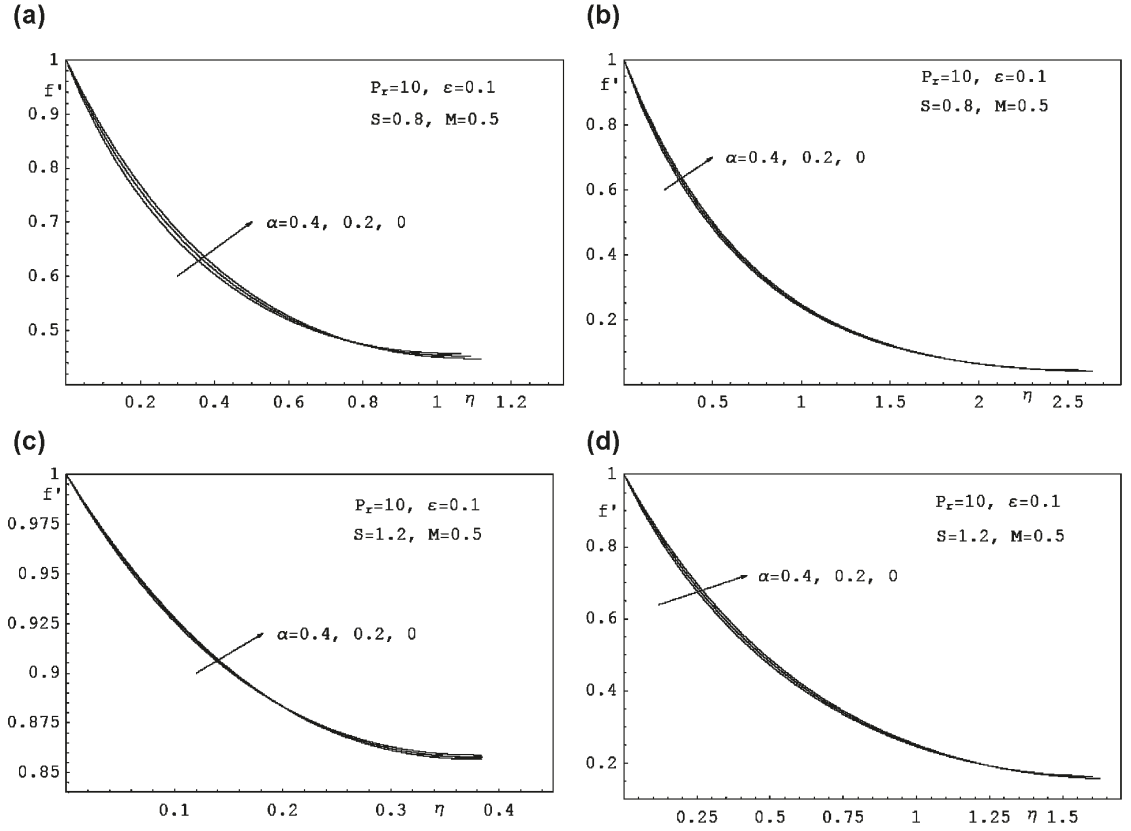

Fig. 4. (*a*) Temperature distribution for various values of ε with $n = 0.8$. (*b*) Temperature distribution for various values of ε with $n = 1.2$. (*c*) Temperature distribution for various values of ε with $n = 0.8$. (*d*) Temperature distribution for various values of ε with $n = 1.2$.

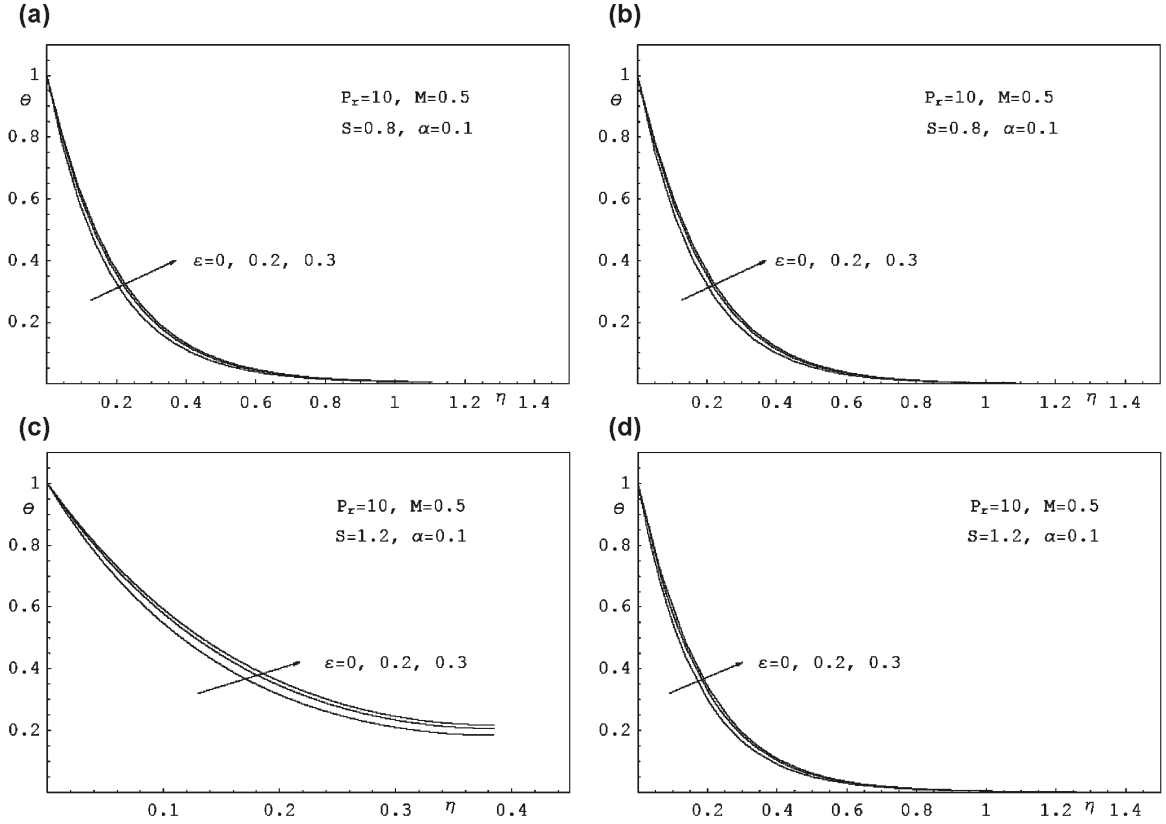

Fig. 5. (*a*) Velocity distribution for various values of M with $n = 0.8$. (*b*) Velocity distribution for various values of M with $n = 1.2$. (*c*) Velocity distribution for various values of M with $n = 0.8$. (*d*) Velocity distribution for various values of M with $n = 1.2$.

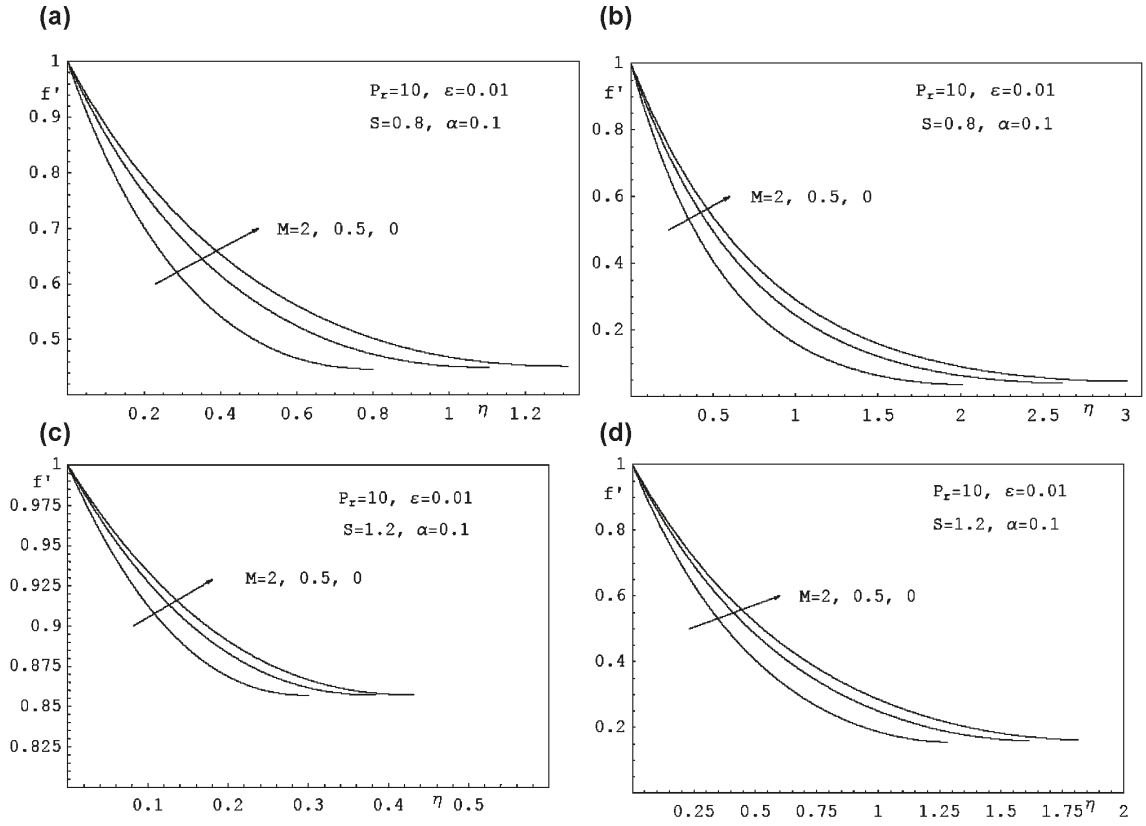

Fig. 6. (*a*) Temperature distribution for various values of M with $n = 0.8$. (*b*) Temperature distribution for various values of M with $n = 1.2$. (*c*) Temperature distribution for various values of M with $n = 0.8$. (*d*) Temperature distribution for various values of M with $n = 1.2$.

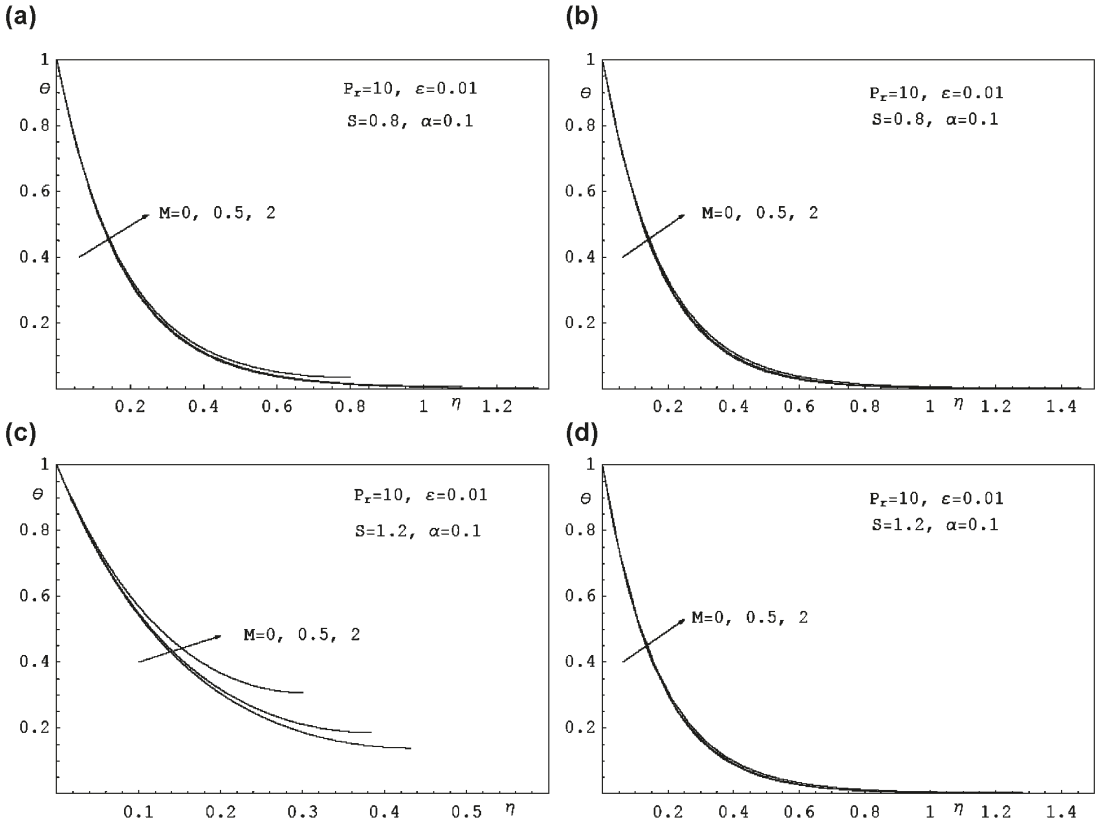

4. Results and discussion

The velocity profiles for various values of the power-law index are presented in Fig. 2. From Figs. 2*a* and 2*b* one observes that for a particular value of the unsteadiness parameter $S = 0.8$ and $S = 1.2$, the velocity decreases as the power-law index n increases and a smaller thickness was observed as the power-law index decreases. This behavior is readily understood from the fact that the pseudo-plastic fluids are more amenable to flow than the dilatant fluids. Also, from Figs. 2*a* and 2*b* , we can observe that as the unsteadiness parameter S increases the thin-film thickness β decreases. Figure 3 illustrates the effect of viscosity parameter α on the velocity profile $f'(\eta)$ where η varies from the stretching sheet ($\eta = 0$) to the free surface of the film ($\eta = \beta$). It can be shown that the film thickness increases as the viscosity parameter decreases. Also, the results show that the velocity increases along the surface with decrease in the viscosity parameter but the reverse is true away from the sheet. The effects of the thermal conductivity ε on the temperature profile θ are presented in Fig. 4. From Fig. 4 , it can be seen that the temperature distribution increases as the thermal conductivity parameter increases. Also, we noticed that the thermal thickness increases as the unsteadiness parameter decreases. Figure 5 shows the effect of the magnetic parameter M on the dimensionless velocity $f'(\eta)$ for two different values of S and two values of n. It is clear that f' decreases as M increases, due to the fact that the Lorentz force, which acts against the flow if the magnetic field, is applied in the normal direction as in our problem. Also, one sees that the film thickness increases with increase in the value of n and decreases with increase in the value of S. The variation of the dimensionless temperature $\theta(\eta)$ within the liquid film for $S = 0.8$, $S = 1.2$, $n = 0.8$, $n = 1.2$ and different values of M are shown in Fig. 6. It should be noted that the dimensionless temperature vanishes at the free surface for $S = 0.8$, $M = 0.0$, and $Pr = 10$. Also, it is observed that θ vanishes for different values of M, $n = 1.2$, $S = 0.8$, and $S = 1.2$. From Fig. 6, it can be seen that the thermal film thickness decreases as S increases for a given value of n. It is clear that the dimensionless temperature increases as M increases. This is because the applied transverse magnetic field produces a drag in the form of the Lorentz force, which opposes the motion and so enhances the temperature. Table 2 presents the values of the local skin-friction coefficient and the local Nusselt number for various values of n, α, ε, and M with Pr. From Table 2 one sees that the local skin-friction coefficient increases as the viscosity parameter increases but the reverse is true for the local Nusselt number. Also, it is observed that both the local skin-friction coefficient and the local Nusselt number decreases as the thermal conductivity parameter increases. The power-law index has the effect of increasing the local skin-friction coefficient and decreasing the local Nusselt number. Also, it is observed that the local Nusselt number decreases with increase in the magnetic parameter while the local skin-friction coefficient increases as M increases.

Table 2. Values of $(-f''(0))^n$ and $-\theta'(0)$ for various values of n, α, M, and ε with $Pr = 10$.

α	S	ε	M	n	$(-f''(0))^n$	$-\theta'(0)$
0	0.8	0.1	0.5	0.8	1.3270	5.3698
0.2	0.8	0.1	0.5	0.8	1.4363	5.3565
0.4	0.8	0.1	0.5	0.8	1.5622	5.3418
0	1.2	0.1	0.5	0.8	0.8996	5.7975
0.2	1.2	0.1	0.5	0.8	0.9267	5.7972
0.4	1.2	0.1	0.5	0.8	0.9604	5.7955
0.1	0.8	0	0.5	0.8	1.3815	5.7179
0.1	0.8	0.2	0.5	0.8	1.3776	5.0629
0.1	0.8	0.3	0.5	0.8	1.3758	4.8045
0.1	1.2	0	0.5	0.8	0.9139	6.1834
0.1	1.2	0.2	0.5	0.8	0.9107	5.4699
0.1	1.2	0.3	0.5	0.8	0.9095	5.1877
0.1	0.8	0.01	0	0.8	1.2289	5.7097
0.1	0.8	0.01	0.5	0.8	1.3814	5.6796
0.1	0.8	0.01	2	0.8	1.7388	5.6067
0.1	1.2	0.01	0	0.8	0.8361	6.1967
0.1	1.2	0.01	0.5	0.8	0.9137	6.1417
0.1	1.2	0.01	2	0.8	1.1046	5.9353
0.1	0.8	0.2	0.5	0.8	1.3776	5.0629
0.1	0.8	0.2	0.5	1	1.4913	5.0185
0.1	0.8	0.2	0.5	1.2	1.5286	4.9758
0.1	1.2	0.2	0.5	0.8	0.9108	5.4699
0.1	1.2	0.2	0.5	1	1.4869	5.4138
0.1	1.2	0.2	0.5	1.2	1.6289	5.3168

5. Conclusions

The influence of the fluid properties, the unsteadiness parameter, and the power-law index on the flow and heat transfer characteristic of an electrically conducting non-Newtonian power-law fluid within a thin liquid film over an unsteady stretching sheet in the presence of a transverse magnetic field have been studied. The results show thatt

(1) the velocity decreases as the magnetic parameter or the power-law index parameter increases and it increases with increase in the unsteadiness parameter.
(2) Near the sheet, the velocity decreases with increase in the viscosity parameter, whereas it increases away from the sheet.
(3) The temperature increases with the increase of the magnetic parameter and the thermal conductivity parameter whereas it decreases as the unsteadiness parameter increases.
(4) The local skin-friction coefficient increases as the viscosity parameter or the power-law index or the magnetic parameter increases and it decreases as the thermal conductivity parameter increases.
(5) The local Nusselt number decreases with an increase of the viscosity parameter, or the thermal conductivity parameter, or the magnetic parameter, or the power-law index increases, whereas it increases as the unsteadiness parameter increases.

Acknowledgements

The authors wish to express thanks to the referee for his valuable comments and suggestions.

References

1. C.Y. Wang. Q. Appl. Math. **48**, 601 (1990).
2. H.I. Andersson, J.B. Aarseh, and B.S. Dandapat. Int. J. Heat Mass Transfer, **43**, 69 (2000). doi:10.1016/S0017-9310(99)00123-4.
3. B.S. Dandapat, B. Santra, and H.I. Andersson. Int. J. Heat Mass Transfer, **46**, 3009 (2003).
4. I.-C. Liu and H.I. Andersson. Int. J. Therm. Sci. **47**, 766 (2008). doi:10.1016/j.ijthermalsci.2007.06.001.
5. M. Subhas Abel, N. Mahesha, and J. Tawade. Appl. Math. Model. **33**, 3430 (2009). doi:10.1016/j.apm.2008.11.021.
6. H.I. Andersson, J.B. Aarseth, N. Braud, and B.S. Dandapat. J. Non-Newtonian Fluid Mech. **62**, 1 (1996). doi:10.1016/0377-0257(95)01392-X.
7. C.-H. Chen. Heat Mass Transfer, **39**, 791 (2003). doi:10.1007/s00231-002-0363-2.
8. C. Wang and I. Pop. J. Non-Newtonian Fluid Mech. **138**, 161 (2006). doi:10.1016/j.jnnfm.2006.05.011.
9. T. Hayat, S. Saif, and Z. Abbas. Phys. Lett. A, **372**, 5037 (2008). doi:10.1016/j.physleta.2008.03.066.
10. A.M. Siddiqui, M. Ahmed, and Q.K. Ghori. Chaos Solitons Fractals, **33**, 1006 (2007). doi:10.1016/j.chaos.2006.01.101.
11. C.-H. Chen. J. Non-Newtonian. Fluid Mech. **135**, 128 (2006). doi:10.1016/j.jnnfm.2006.01.009.
12. B.S. Dandapat, B. Santra, and K. Vajravelu. Int. J. Heat Mass Transfer, **50**, 991 (2007). doi:10.1016/j.ijheatmasstransfer.2006.08.007.
13. M. Massoudi and T.X. Phuoc. Contin. Mech. Thermodyn. **16**, 529 (2004). doi:10.1007/s00161-004-0178-0.
14. M.A.A. Mahmoud. Can. J. Chem. Eng. **87**, 47 (2009). doi:10.1002/cjce.20135.
15. T.C. Chiam. Acta Mech. **129**, 63 (1998). doi:10.1007/BF01379650.
16. M.A. Hossain, M.S. Munir, and D.A.S. Rees. Int. J. Therm. Sci. **39**, 635 (2000). doi:10.1016/S1290-0729(00)00227-1.
17. T.C. Chiam. Int. Commun. Heat Mass Transf. **23**, 239 (1996). doi:10.1016/0735-1933(96)00009-7.
18. M.S. Abel and N. Mahesha. Appl. Math. Model. **32**, 1965 (2008). doi:10.1016/j.apm.2007.06.038.
19. M.A.A. Mahmoud. Physica A, **375**, 401 (2007). doi:10.1016/j.physa.2006.09.010.